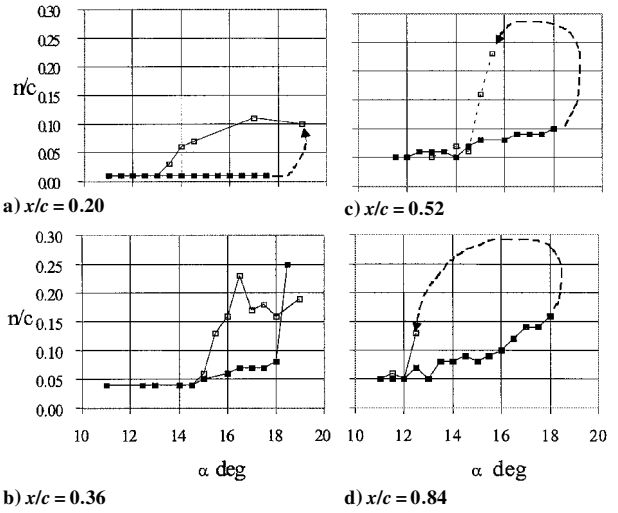

Fig. 2 Variation of the vortical layer thickness during the oscillation cycle: Filled symbols denote pitch up, and open symbols denote pitch down.

and then jumps to 25% of the chord at u18.5 deg. This corresponds to the arrival of the reversed-flow region (SLV) in its upstream movement along the airfoil surface. The results at $x/c = 0.52$ and 0.84 (Figs. 2c and 2d) show a similar trend, differing only in the timing of the events. In each case, the initial viscous layer, which is already quite thick, further thickens as the incidence increases to u18.0 deg. At this point it is no longer possible to define a vortical layer thickness because the boundary of the vortical layer has moved outside the visualization field. In each case, during the downward pitching phase of the oscillation, the flow recovers, completing the hysteresis loop, even though only a part of the thumb curve lies within the field of vision.

Conclusions

The present investigation of the oscillating airfoil showed that, under the operating conditions studied, the airfoil undergoes light dynamic stall. This stall process is characterized by the formation, growth, and upstream movement of a vortical layer in the aft region of the airfoil, leading to large-scale flow separation and eventual shedding of a weak vortex, the so-called SLV. No LEV formation or the scenario associated with deep stall was observed during the pitch-up motion. The initiation of the stall process from the trailing edge is believed to be characteristic of the NACA 0015 airfoil section tested. The experiments also indicated strong hysteresis effects in the flow evolution. The present velocity data are consistent with pressure and lift measurements on oscillating NACA 0015 airfoils reported in the literature.

References

[1]McCroskey, W. J., "Unsteady Airfoils," *Annual Review of Fluid Mechanics*, Vol. 14, 1982, pp. 285–311.

[2]Raffel, M., "PIV-Messungen instationärer Geschwindigkeitfelder an einem schwingenden Rotorprofil," DLR, Rept. DLR-FB-93-50, Göttingen, Germany, Oct. 1993.

[3]Oshima, H., and Ramaprian, B. R., "Velocity Measurements over a Pitching Airfoil," *AIAA Journal*, Vol. 35, No. 1, 1997, pp. 119–126.

[4]Piziali, R. A., "2-D and 3-D Oscillating Wing Aerodynamics for a Range of Angles of Attack Including Stall," NASA TM-4632, Sept. 1994.

[5]O'Gorman, L., and Sanderson, A., "The Converging Squares Algorithm: An Efficient Method for Locating Peaks in Multidimensions," *IEEE Transactions on Pattern Analysis and Machine Intelligence*, Vol. 8, No. 3, 1984, pp. 280–288.

[6]Rank, M., "PIV Study of the Two-Dimensional Flow Field Around an Oscillating Airfoil," M.S. Thesis, School of Mechanical and Materials Engineering, Washington State Univ., Pullman, WA, Dec. 1997.

A. Plotkin
Associate Editor

Effect of Thickness on Large-Deflection Behavior of Shells

Reaz A. Chaudhuri* and Raymond L. Hsia†
University of Utah, Salt Lake City, Utah 84112

Introduction

INVESTIGATIONS pertaining to the effect of transverse shear/normal deformation on the large-deflection behavior of moderately thick shells appear to be absent in the literature, although such an effect has been thoroughly investigated in the small-deflection regime (see, e.g., Ref. 1). The primary objective of the present research is to investigate thoroughly the combined effects of geometric nonlinearity and transverse shear/normal deformation on the large elastic deformation behavior of moderately thick shells and panels of finite dimensions. Second, the question of what the Kirchhoff hypothesis means in the nonlinear regime still remains unsettled. Obviously, it cannot be the same as its linear counterpart. This triggered our interest in developing the fully nonlinear kinematic formulation for moderately thick shells as opposed to its von Kármán counterpart.

The present analysis accounts for all of the nonlinear terms in the kinematic relations and utilizes the total Lagrangian formulations in incremental equilibrium equations. A nonlinear, moderately thick shell, finite element methodology is developed to obtain the discretized system equations. The element is capable of accurately modeling the curved geometry of a shell, taking advantage of a tensorial formulation that uses the surface-parallel curvilinear coordinates of non-Euclidean geometry. The present nonlinear finite element solution methodology is based on a quasi-three-dimensional hypothesis known as linear displacement distribution through thickness (LDT) theory.[2] A curvilinear-side, 24-node element with 12 nodes on each of the top and bottom surfaces of a shell is implemented to model the quasi-three-dimensional interlaminar deformation behavior represented by the LDT. The Broyden–Fletcher–Goldfarb–Shanno (BFGS) iterative scheme[3] is used to solve the resulting nonlinear equations. A thin/shallow clamped cylindrical panel is investigated to test the convergence of the present element and to compare the present solution with the available numerical results. The convergence rate of the present serendipity-type cubic element is compared with that of its quadratic counterpart. Additionally, numerical results for shallow clamped cylindrical panels are presented to provide new insights into certain interesting deformation behaviors of thick and thin homogeneous isotropic cylindrical panels in the advanced nonlinear regimes. The relative (to linear) nonlinear membrane-to-shear effect, defined as the ratio of normalized deflections computed using the nonlinear and linear analyses, studied here for the first time, sheds new light on the relative roles of transverse shear/normal deformation and surface parallel membrane effects in thin to thick shell regimes.

Isoparametric Finite Element Discretization

The convected coordinates of a generic point (x^1, x^2, z) in an element with 12 nodal points on each of the top and bottom surfaces are, in terms of the natural coordinates r, s given by

$$x^j(r,s,z) = \left(1 - \frac{z}{h}\right)\sum_{k=1}^{12}\psi_k(r,s)_b x_k^j + \frac{z}{h}\sum_{k=1}^{12}\psi_k(r,s)_t x_k^j$$

$$\text{for} \qquad j = 1, 2 \quad \text{(1a)}$$

Received April 3, 1997; revision received Sept. 18, 1998; accepted for publication Oct. 6, 1998.

*Associate Professor, Department of Materials Science and Engineering. E-mail: R.Chaudhuri@m.cc.utah.edu.

†Graduate Research Assistant, Department of Civil Engineering; currently Assistant Squad Leader, Structures Division, Utah Department of Transportation, Salt Lake City, UT 84119.

$$z(r,s,z) = \left(1 - \frac{z}{h}\right)\sum_{k=1}^{12}\psi_k(r,s)_b z_k + \frac{z}{h}\sum_{k=1}^{12}\psi_k(r,s)_t z_k \quad (1b)$$

where $\psi_k(r,s)$ are the interpolation functions taking a value of unity at nodes k and zero at all other nodes. The quantities ${}_bx_k^1$, ${}_bx_k^2$, ${}_bz_k$ and ${}_tx_k^1$, ${}_tx_k^2$, ${}_tz_k$ are coordinates of the nodal point k on the bottom and top surfaces of the shell, respectively. In the linear displacement theory, the incremental displacements of the shell are given by

$$\{{}_ov\} = [T_{BT}(z)][\phi(r,s)]\{{}_oV_{BT}\} \quad (2)$$

in which $[T_{BT}(z)]$ is the linear (through the thickness) matrix operator[2] and the nodal displacement vector $\{{}_oV_{BT}\}$ of the shell is defined by

$$\{{}_oV_{BT}\}^T = \{{}_oU_{b1}\cdots\cdots{}_oW_{b12} \quad {}_oU_{t1}\cdots\cdots{}_oW_{t12}\} \quad (3)$$

where the quantities ${}_oU_{bk}$, ${}_oV_{bk}$, ${}_oW_{bk}$ and ${}_oU_{tk}$, ${}_oV_{tk}$, ${}_oW_{tk}$, $k = 1, \ldots, 12$, are the incremental displacements of the nodal point k on the top and bottom surfaces of the shell in the x^1, x^2, z directions, respectively, at time t; and

$$[\Phi(r,s)] = \begin{bmatrix} \{\psi\} & \{0\} & \{0\} & \{0\} & \{0\} & \{0\} \\ \{0\} & \{\psi\} & \{0\} & \{0\} & \{0\} & \{0\} \\ \{0\} & \{0\} & \{\psi\} & \{0\} & \{0\} & \{0\} \\ \{0\} & \{0\} & \{0\} & \{\psi\} & \{0\} & \{0\} \\ \{0\} & \{0\} & \{0\} & \{0\} & \{\psi\} & \{0\} \\ \{0\} & \{0\} & \{0\} & \{0\} & \{0\} & \{\psi\} \end{bmatrix} \quad (4)$$

where $\{\psi\} = \{\psi_1\ \psi_2\ \psi_3\ \psi_4\ \psi_5\ \psi_6\ \psi_7\ \psi_8\ \psi_9\ \psi_{10}\ \psi_{11}\ \psi_{12}\}$ and $\{0\}$ is 1×12 null matrix; $\psi_k(r,s)$, $k = 1, \ldots, 12$, are the same interpolation functions used in Eqs. (1). The details of the nonlinear kinematic relations and the related development of the finite element equations are available from Hsia and Chaudhuri[2] and Kim and Chaudhuri[4] and are not repeated here in the interest of brevity of presentation. Notations are also identical to those of the earlier papers.

The stiffness matrices and force vectors are computed using the full numerical integration scheme, i.e., $3 \times 3 \times 2$ Gaussian integration points. Note that the twin phenomena of shear and membrane locking encountered by thick/deep shell elements, such as the present one, can be avoided either by use of higher-order elements[5] or by employment of reduced/selective numerical integration schemes.

Example: Analysis of Isotropic Clamped Thin and Thick Cylindrical Panels Under Uniform Loading

An isotropic, thin shallow cylindrical panel of uniform thickness (Fig. 1) is investigated for the purpose of comparison of the present results with those of other investigators. Additionally, this problem has been selected to test the performance of the present surface-parallel cubic, 24-node element especially with regard to shear and membrane lockings. (Note in this connection that a concentrated force cannot be applied in a three-dimensional problem such as the present one because such a force is, according to the three-dimensional linear elasticity theory, known to yield singular displacement and stress distributions at its point of application; see, e.g., Ref. 6. Such singular displacement and stress distributions also persist in its nonlinear counterpart, although this has, to the authors' knowledge, not been explored in the literature.)

The geometric and material property data are listed in Fig. 1. The panel is rigidly clamped along all four boundaries so that all of the displacement components, u, v, and w, vanish at the edges of the panel (C2 boundary conditions). The top (outward) surface of the panel is subjected to uniform inward radial loading. Double-symmetry conditions permit every model under consideration to be limited to only a quarter of the geometry, such that the corresponding surface-parallel displacements vanish along the centerlines and the deformed shapes are assumed to be symmetric. In this study, the surface aspect ratio of each shell element is kept close to 1 for

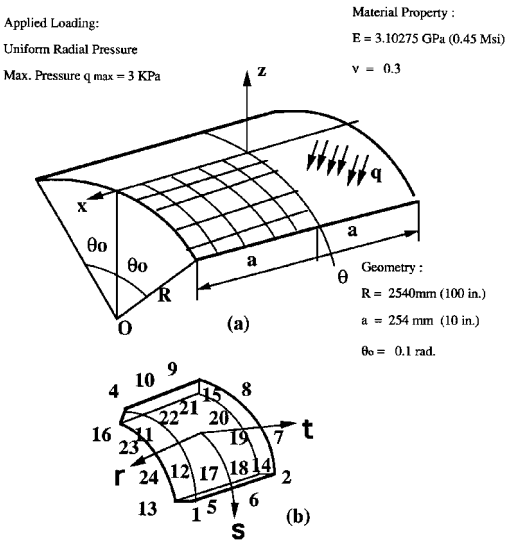

Fig. 1 Geometric model of a) clamped cylindrical panel under uniformly distributed loading and b) a 24-node, curvilinear side, surface-parallel cubic serendipity-type isoparametric element.

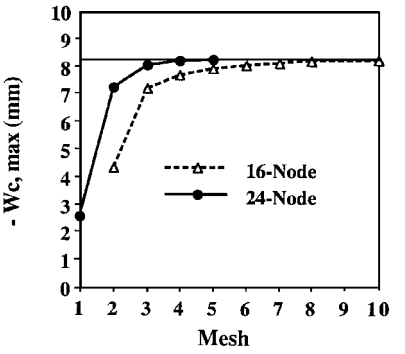

Fig. 2 Comparison of convergence between the present serendipity-type, 24-node cubic element and its 16-node quadratic counterpart.

numerical reasons, in order to ensure uniform convergence of displacement in the surface-parallel directions. The pressure load is carried well into the advanced nonlinear region.

First, convergence of the present surface-parallel cubic, 24-node, serendipity-type quadrilateral shell element is shown in Fig. 2, where the central deflection w_c of an isotropic cylindrical panel of thickness $h = 2.54$ mm vs the number of divisions is plotted for the maximum uniform radial pressure $[P_r^{(t)} = -q_{\max};\ P_r^{(b)} = 0]$. No shear locking has been observed that can cause significant deterioration of the performance of the present cubic 24-node element. Severe membrane locking is not expected in a large-deflection problem such as the one under consideration, even for a very shallow (almost flat) panel, because, unlike its linear counterpart, geometric nonlinearity always produces membrane stresses in the large-deflection regime. As regards shear locking, note that in the nonlinear regime the transverse shear deformation is coupled to the surface-parallel membrane effect, which prevents development of severe shear locking even in a very thin panel. Additionally, as was pointed out by Bathe and Bolourchi,[5] no reduced integration scheme need be employed for higher-order elements such as the present one.

A comparison of results obtained using cubic (24-node) and quadratic (16-node) elements of a homogeneous isotropic shallow thin panel is shown in Fig. 2, which clearly demonstrates superiority of the 24-node cubic element to its quadratic 16-node counterpart in regard to rapidity of convergence. A 3×3 cubic element mesh is adequate to achieve the same level of convergence, which can be attained by a 6×6 quadratic element mesh, which makes the former possibly one of the most numerically efficient, yet accurate, shell elements formulated and coded to date. The results shown in Fig. 2

Table 1 Relative (to linear) nonlinear membrane-to-shear effect in clamped isotropic cylindrical panels

Ratio, $2a/h$	$(W_c^*)_1$ (at 1st step)	$(W_c^*)_{60}$ (at 60th step)	$\frac{(W_c^*)_{60}}{(W_c^*)_1}$
2	0.40626	0.39792	0.9795
4	0.15139	0.15136	0.9998
5	0.12193	0.12196	1.0002
8	0.08883	0.08886	1.0003
10	0.08048	0.08050	1.0003
20	0.06482	0.06493	1.0016
25	0.06025	0.06055	1.0049
32	0.05358	0.05435	1.0144
40	0.04810	0.04983	1.0359
50	0.04087	0.04433	1.0847

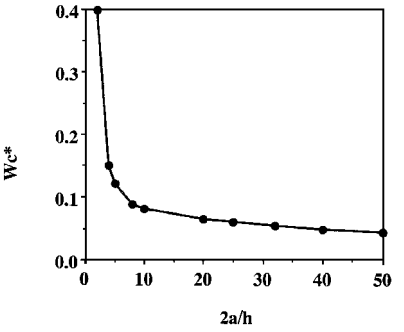

Fig. 3 Effect of thickness on the normalized deflection of clamped cylindrical panels.

reveal that the displacements converge reasonably rapidly for the maximum central deflection computed using the 3×3 mesh to be in error of 2.45% with respect to its 5×5 counterpart. The relative percentage of error is computed with respect to the 5×5 mesh of the present cubic element.

Figure 3 shows the variation of the normalized central deflection W_c^*, defined by

$$W_c^* = \frac{100Eh^3 w_c}{q(2a)^4} \tag{5}$$

with respect to the length-to-thickness ratio $2a/h$. Figure 3 clearly indicates that the (three-dimensional) effect of transverse shear/normal deformation is significant for panels of length-to-thickness ratio lower than 10. Table 1 shows comparisons between normalized deflections computed using linear and nonlinear analyses. Normalized linear deflection is computed from the results obtained using the first load step. The ratio of normalized deflections computed using the nonlinear and linear analyses, termed the relative (to linear) nonlinear membrane-to-shear effect $(W_c^*)_{60}/(W_c^*)_1$, also is presented in Table 1. The normalized deflection computed using the nonlinear analysis is about 2% smaller than its linear counterpart when the length-to-thickness ratio is 2. Both the linear and nonlinear normalized deflections are almost equal in the case of a cylindrical panel of length-to-thickness ratio equal to 5. Beyond this, the nonlinear normalized deflection is larger than its linear counterpart. For example, normalized deflection computed using the nonlinear analysis is about 8.5% larger than its linear counterpart when the length-to-thickness ratio is 50. The reason for the difference is that, in a thinner panel, the nonlinear membrane effect is stronger than in the case of a thicker panel.

Conclusions

The isoparametric, surface-parallel, serendipity-type cubic element developed under the framework of fully nonlinear transverse shear and normal deformation can be used effectively to model the deformation behavior of thin to moderately thick shell structures in the advanced nonlinear regime, while leaving the general form of the element stiffness matrix unchanged relative to the C^o-type, three-dimensional elasticity elements. Thus, it may be incorporated easily into existing structural analysis programs. The 24-node cubic serendipity element appears to be one of the most accurate, yet computationally efficient, shell elements developed for this purpose.

Numerical results for isotropic thick/shallow cylindrical panels clearly indicate that the (three-dimensional) effect of nonlinear transverse shear and normal deformation is, like its linear counterpart, significant for panels of length-to-thickness ratio lower than 10.

Numerical results for isotropic cylindrical panels show that normalized deflection computed using the nonlinear analysis is slightly smaller than its linear counterpart when the length-to-thickness ratio is less than 5. Beyond this, the nonlinear normalized deflection becomes increasingly larger than its linear counterpart. The reason for the difference is that, in a thinner panel, the nonlinear membrane effect is stronger than in the case of a thicker panel. The deformation of thicker cylindrical panels is dominated primarily by the transverse shear and normal strains, which are negligible in thinner panels, such as $2a/h \geq 50$.

References

[1]Seide, P., and Chaudhuri, R. A., "Triangular Finite Element for Analysis of Thick Laminated Shells," *International Journal for Numerical Methods in Engineering*, Vol. 24, No. 8, 1987, pp. 1563–1579.

[2]Hsia, R. L., and Chaudhuri, R. A., "Geometrically Nonlinear Analysis of Cylindrical Shells Using Surface-Parallel Quadratic Elements," *Computers and Structures*, Vol. 61, No. 6, 1996, pp. 1143–1154.

[3]Matthies, H., and Strang, G., "The Solution of Nonlinear Finite Element Equations," *International Journal for Numerical Methods in Engineering*, Vol. 14, 1979, pp. 1613–1626.

[4]Kim, D., and Chaudhuri, R. A., "Full and von Kármán Geometrically Nonlinear Analyses of Laminated Cylindrical Panels," *AIAA Journal*, Vol. 33, No. 11, 1995, pp. 2173–2181.

[5]Bathe, K. J., and Bolourchi, S., "A Geometric and Material Nonlinear Plate and Shell Element," *Computers and Structures*, Vol. 11, Nos. 1–2, 1980, pp. 23–48.

[6]Sokolnikoff, I. S., *Mathematical Theory of Elasticity*, 2nd ed., McGraw–Hill, New York, 1956, Secs. 90, 91.

A. M. Waas
Associate Editor